tances of the two occupied cavities, Rh(1,3,4,5) and Rh(8,9,10,12), average to 2.78(1) Å, whereas the 16 surface Rh–Rh distances of the four unoccupied cavities average to 2.75(1) Å. This represents a 1% expansion in the dimensions of filled holes relative to empty holes and is consistent with (but smaller than) the 2 to 3% expansion deduced from earlier x-ray work (6). Studies on the binary Rh-H system also support an increase in metal-metal distance upon occupation of a cavity by H, with expansions typically in the 5% range [see S. Wilke, D. Hennig, R. Löber, *Phys. Rev. B* **50**, 2548 (1994)].

19. K. Christmann, *Prog. Surf. Sci.* **48**, 15 (1995); *Mol. Phys.* **66**, 1 (1989).
20. Although there have not been any structural results of H-Rh(100) derived from LEED or He scattering 544 (1991); G. Parschau, E. Kirsten, K. H. Rieder, *Phys. Rev. B* **43**, 12216 (1991); K. Christmann, M. Ehsasi, W. Hirshwald, J. H. Block, *Chem. Phys. Lett.* **131**, 192 (1986).
22. L. J. Richter and W. Ho, *J. Vac. Sci. Technol. A* **5**, 453 (1987).
23. D. R. Hamann and P. J. Feibelman, *Phys. Rev. B* **37**, 3847 (1987); P. J. Feibelman and D. R. Hamann, *Surf. Sci.* **234**, 377 (1990); P. J. Feibelman, *Phys. Rev. B* **43**, 9452 (1991); D. Hennig, S. Wilke, R. Löber, M. Methfessel, *Surf. Sci.* **287-288**, 89 (1993).
24. Although the rate of diffusion of H in Rh has not (as far as we know) been measured, one can cite as a representative example the value of 2×10^{12} jumps per second for the diffusivity of H in V at room temperature [see J. Völkl and G. Alefeld, in [T. Eguchi *et al.*, *J. Chem. Soc. Dalton Trans.* **1996**, 625 (1996)].
26. A. Bashall *et al.*, *Angew. Chem. Int. Ed. Engl.* **30**, 1164 (1991).
27. B. T. Heaton *et al.*, *J. Chem. Soc. Dalton Trans.* **1982**, 1499 (1982).
28. D. Hanke *et al.*, *Inorg. Chem.* **32**, 4300 (1993).
29. M. J. Fernandez *et al.*, *J. Am. Chem. Soc.* **106**, 5458 (1984).
30. R. K. Brown, J. M. Williams, A. J. Sivak, E. L. Muetterties, *Inorg. Chem.* **19**, 370 (1980).
31. J. S. Ricci, T. F. Koetzle, R. J. Goodfellow, P. Espinet, P. M. Maitlis, *ibid.* **23**, 1828 (1984).
32. This research was supported by NSF grant CHE-9421769, American Chemical Society grant PRF-

Probing Single Molecules and Single Nanoparticles by Surface-Enhanced Raman Scattering

Shuming Nie* and Steven R. Emory

Optical detection and spectroscopy of single molecules and single nanoparticles have been achieved at room temperature with the use of surface-enhanced Raman scattering. Individual silver colloidal nanoparticles were screened from a large heterogeneous population for special size-dependent properties and were then used to amplify the spectroscopic signatures of adsorbed molecules. For single rhodamine 6G molecules adsorbed on the selected nanoparticles, the intrinsic Raman enhancement factors were on the order of 10^{14} to 10^{15}, much larger than the ensemble-averaged values derived from conventional measurements. This enormous enhancement leads to vibrational Raman signals that are more intense and more stable than single-molecule fluorescence.

Recent advances in ultrasensitive instrumentation have allowed the detection, identification, and dynamic study of single molecules in low-temperature solids (*1–3*), in room-temperature liquids (*4*, *5*), and on dielectric surfaces (*6–9*). This capability opens many opportunities for scientists in various disciplines such as analytical chemistry, molecular biology, and nanostructured materials (*10–12*). Current methods for probing single molecules, however, are restricted to a few basic principles. These mainly include laser-induced fluorescence with near-field, far-field, and evanescent-wave excitation, frequency-modulated optical absorption at low temperatures (*1*, *2*), and electrochemical detection of redox-active species (*13*). We report a methodology based on surface-enhanced Raman scattering (SERS) (*14*) for studying single molecules adsorbed on single nanoparticles at room temperature. By coupling single molecules to nanoparticles, we demonstrated that nanometer-sized particles can amplify the spectroscopic signatures of single molecules enormously and that the size-dependent properties of nanostructures can be examined at the single-particle level.

Single-molecule detection by SERS is expected to extend and complement fluorescence studies. Except in low-temperature solids (*15*), fluorescence measurements do not provide detailed molecular information, and photobleaching often limits the number of photons obtainable from a single molecule. These problems could be overcome with the use of Raman spectroscopy, which is capable of providing highly resolved vibrational information and does not suffer from rapid photobleaching. However, Raman scattering is an extremely inefficient process, and its cross sections ($\sim 10^{-30}$ cm^2 per molecule) are about 14 orders of magnitude smaller than those of fluorescent dyes ($\sim 10^{-16}$ cm^2 per molecule). To achieve single-molecule detection sensitivity, the normal efficiency of Raman scattering must be enhanced 10^{14}-fold or more. We demonstrate that such enormous degrees of signal amplification can be obtained by exploiting the surface-enhanced Raman effect and the resonance enhancement effect. Recently, Kneipp *et al.* (*16*) reported similar magnitudes of surface enhancement and detected single-molecule Raman signals with near-infrared laser excitation.

An unexpected finding during this work was that a very small number of nanoparticles exhibited unusually high enhancement efficiencies. These particles emitted bright, Stokes-shifted (toward longer wavelengths) light and are called "hot particles." To screen for these hot particles in a heterogeneous Ag colloid solution, we incubated an aliquot of the colloid with rhodamine 6G (R6G) molecules for an extended period of time (~3 hours) at room temperature. The colloidal particles were immobilized on polylysine-coated glass surfaces because of the electrostatic interactions between the negative charges on the particles and the positive charges on the surface (*17*). Other methods using organosilane and thiol compounds are also available for immobilizing and dispersing colloidal particles on surfaces (*18*). Morphological studies by transmission electron microscopy and atomic force microscopy (AFM) showed that the colloid was a mixture of heterogeneous particles with an average particle size of about 35 nm and a typical concentration of $\sim 10^{11}$ particles/ml. With wide-field laser illumination, about 200 to 1000 immobilized particles were examined in one field of view or a 100 μm × 100 μm

Department of Chemistry, Indiana University, Bloomington, IN 47405, USA.

*To whom correspondence should be addressed. E-mail: nie@indiana.edu

sampling area. A small number of the particles emitted light at longer wavelengths relative to the laser line. The laser scattering and Stokes-shifted signals of immobilized Ag particles were recorded directly on color photographic film (Fig. 1). Although superficially similar to fluorescence, spectroscopic measurement of individual particles with a diffraction-limited, confocal laser beam reveals that the observed signals arise from Raman scattering of adsorbed R6G. Fluorescence line narrowing can be ruled out because we are able to obtain vibrational spectra from nonfluorescent biomolecules (that is, tryptophan derivatives) and pyridine compounds adsorbed on single Ag particles. Furthermore, the fluorescence emission of R6G is quenched by rapid energy transfer from the excited electronic state to the metal surface. On the basis of the measured adsorption isotherms (*19*), we estimate that about 80% of R6G molecules are adsorbed on Ag particles and that each particle carries an average of one analyte molecule at a R6G concentration of 2×10^{-10} M and an average of 0.1 molecule at 2×10^{-11} M. The number of observed hot particles increases with the R6G concentration, but the relation is not linear. A likely reason is that the number of intrinsically hot particles is far smaller than that of the analyte molecules even at these low concentrations. Most of the R6G molecules are thus adsorbed on inactive particles and are not detected.

A common practice in bulk SERS studies has been to activate the colloid by electrolyte-induced aggregation (*14*). The activated colloid contains large clusters of particles, which are believed to be the most efficient for Raman enhancement. However, intense Raman signals can also be obtained from Ag colloids that are activated, but not aggregated, by <1 mM chloride ions (*19*). To determine whether the optically hot particles were single particles or aggregates, we carried out correlated optical and topographic studies of the immobilized nanoparticles using an integrated optical and atomic force microscope (*20*). High-resolution AFM images of selected hot Ag nanoparticles (Fig. 2) show that the majority of them are well-separated, single particles with a narrow size range of 110 to 120 nm in diameter, indicating a strong correlation between enhancement efficiency and particle size. A minor fraction consists of aggregates, each containing two to six tightly packed particles. However, it is not clear whether aggregation causes the efficient Raman enhancement or if a hot particle happens to be trapped in the aggregate (*21*). The correlation with particle shape appears to be weak because no consistent shape has been found in the examined hot particles.

Several lines of evidence indicate that the observed SERS signals arise from single adsorbed molecules (or conjugated molecular aggregates that behave as single molecules). At analyte concentrations below 10^{-10} M, single colloidal particles are expected to contain mostly zero or one analyte molecule according to a Poisson distribution. This criterion has been widely used in fluorescence detection of single molecules in homogeneous liquids (*5*). However, the colloid system was highly heterogeneous, and most particles did not exhibit efficient Raman enhancement. As measured in situ by AFM, the optically hot particles were about three times the average particle size and thus likely to have nine times the average surface area. Also, it is not known whether the hot particles contain adsorption sites or facets of unusually high affinities, which could preferentially accumulate R6G molecules onto these particles.

Strong evidence has been obtained from Raman polarization measurements at the single-particle level. The surface-immobilized nanoparticles have random orientations, similar to randomly oriented molecules on a glass or polymer surface (*6–8*). Excitation-polarization data were obtained from two particles under identical conditions (Fig. 3). These two particles were selected to show that intense Raman signals can be observed with either s- or p-polarized light (parallel or perpendicular to the plane of incidence), depending on how a particular particle is oriented relative to the polarization axis. From the electromagnetic theory of surface plasmon resonance (*14*), these two nanoparticles should have orthogonal orientations: When one is maximally excited at the direction of s polarization, the other is minimally excited, and vice versa. We believe that the overall excitation polarization contains two contributions: one from the preferential excitation of an oriented nanoparticle, and the other from the preferential excitation of the Raman polarizability tensors of an oriented

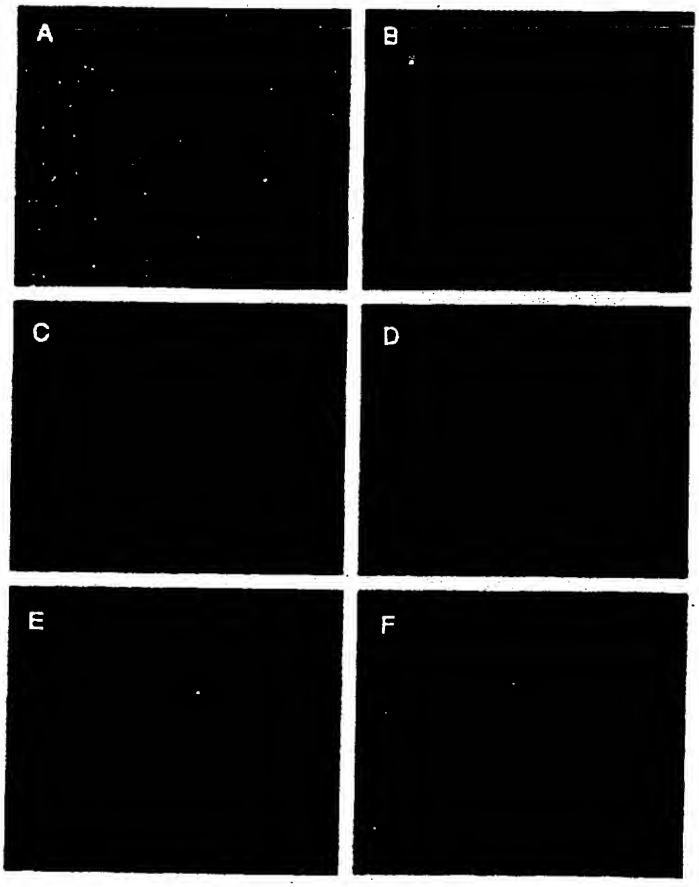

Fig. 1. Single Ag nanoparticles imaged with evanescent-wave excitation. Total internal reflection of the laser beam at the glass-liquid interface was used to reduce the laser scattering background. The instrument setup for evanescent-wave microscopy was adapted from Funatsu *et al.* (*11*). The images were directly recorded on color photographic film (ASA-1600) with a 30-s exposure by a Nikon 35-mm camera attached to the microscope. (**A**) Unfiltered photograph showing scattered laser light from all particles immobilized on a polylysine-coated surface. (**B**) Filtered photographs taken from a blank Ag colloid sample (incubated with 1 mM NaCl and no R6G analyte molecules). (**C**) and (**D**) Filtered photographs taken from a Ag colloid sample incubated with 2×10^{-11} M R6G. These images were selected to show at least one Raman scattering particle. Different areas of the cover slip were rapidly screened, and most fields of view did not contain visible particles. (**E**) Filtered photograph taken from Ag colloid incubated with 2×10^{-10} M R6G. (**F**) Filtered photograph taken from Ag colloid incubated with 2×10^{-9} M R6G. A high-performance bandpass filter was used to remove the scattered laser light and to pass Stokes-shifted Raman signals from 540 to 580 nm (920 to 2200 cm^{-1}). Continuous-wave excitation at 514.5 nm was provided by an Ar ion laser. The total laser power at the sample was 10 mW. Note the color differences between the scattered laser light in (A) and the red-shifted light in (C) through (F).

molecule. These two components can be separated by using polarization-scrambled laser excitation and detecting Raman emission with a dichroic polarizer (Fig. 4). The polarized data are in direct contrast with previous measurements, which show that bulk SERS spectra are strongly depolarized (*14*).

Similar to the fluorescence study of single molecules (*6–9*), Raman polarization data allow the orientation of a single molecule to be determined. The intense Raman signals at about 1657, 1578, 1514, 1365, 1310, and 1184 cm^{-1} arise from the totally symmetric modes of in-plane C-C stretching vibrations. These vibrational frequencies are similar to solution resonance Raman and bulk surface-enhanced Raman spectra of R6G (within 3 to 4 cm^{-1}), although the relative spectral intensities are considerably different. The strong electronic transition excited at 514.5 nm is polarized in the direction of the long molecular axis of R6G, and the intense Raman lines are all described by a single component (α_{xx}) of the scattering tensor along this axis (*22*). If R6G adsorbs on the Ag surface in a tilted, edge-on configuration (*19*), the molecule measured in Fig. 4 should have its long molecular axis parallel with the polarizer (upper spectrum).

Further evidence for single-molecule behavior comes from the observation of sudden spectral changes. Photochemical decomposition or photobleaching is significantly reduced for single molecules adsorbed on metal nanoparticles because the metal surface rapidly quenches the excited electronic state and thus prevents excited-state reactions. However, the Raman signals do suddenly disappear or change after a few minutes of continuous illumination. In a series of Raman spectra taken from a single particle at different times (Fig. 5), the observed changes in Raman signal frequencies are as large as 10 cm^{-1}. This finding resembles fluorescence spectral diffusion observed for single molecules in low-temperature solids (*1*). Even when sudden spectral changes are not observed, the Raman spectra obtained from different particles have slightly different vibrational frequencies (Figs. 3 and 4), suggesting that each molecule is adsorbed at a different site.

These single-molecule, single-particle results indicate that the intrinsic enhancement factors in SERS can be as high as 10^{14} to 10^{15}, yielding Raman scattering cross sections on the order of 10^{-15} cm^2 per molecule. This value is comparable with or higher than the optical cross sections of single-chromophore fluorescent dyes. For a more direct comparison, we measured the relative fluorescence and Raman signals from single R6G molecules under the same

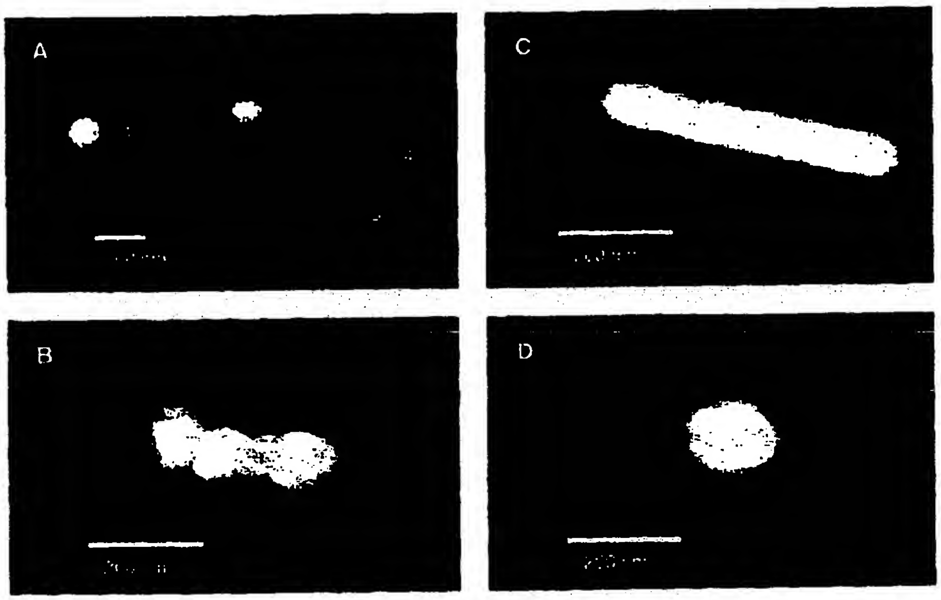

Fig. 2. Tapping-mode AFM images of screened Ag nanoparticles. **(A)** Large area survey image showing four single nanoparticles. Particles 1 and 2 were highly efficient for Raman enhancement, but particles 3 and 4 (smaller in size) were not. **(B)** Close-up image of a hot aggregate containing four linearly arranged particles. **(C)** Close-up image of a rod-shaped hot particle. **(D)** Close-up image of a faceted hot particle.

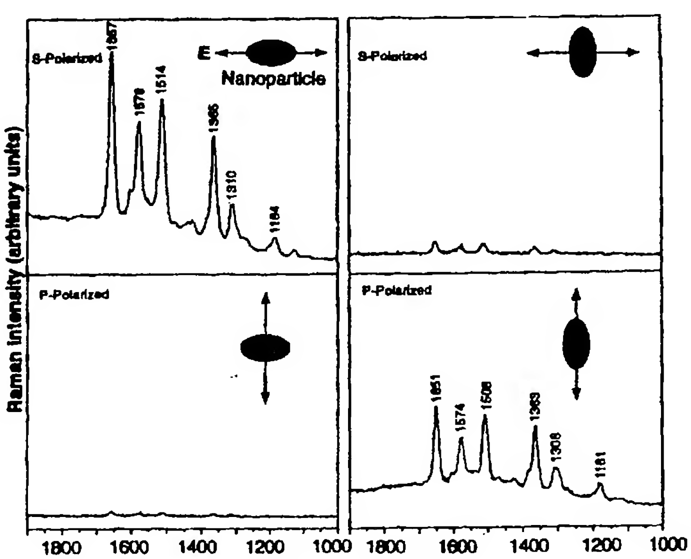

Fig. 3. Surface-enhanced Raman spectra of R6G obtained with a linearly polarized confocal laser beam from two Ag nanoparticles. The R6G concentration was 2 × 10^{-11} M, corresponding to an average of 0.1 analyte molecule per particle. The direction of laser polarization and the expected particle orientation are shown schematically for each spectrum. Laser wavelength, 514.5 nm; laser power, 250 nW; laser focal radius, ~250 nm; integration time, 30 s. All spectra were plotted on the same intensity scale in arbitrary units of the CCD detector readout signal.

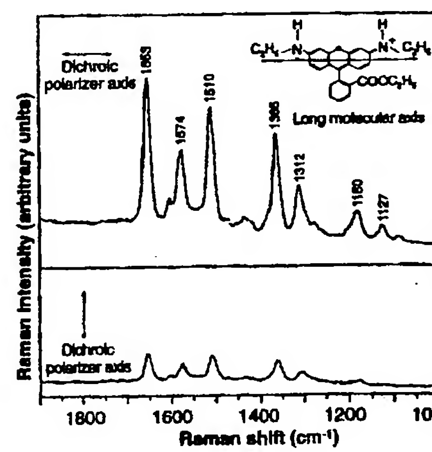

Fig. 4. Emission-polarized surface-enhanced Raman signals of R6G observed from a single Ag nanoparticle with a polarization-scrambled confocal laser beam. A dichroic sheet polarizer was rotated 90° to select Raman scattering signals polarized parallel (upper spectrum) or perpendicular (lower spectrum) to the long molecular axis of R6G. **(Inserts)** Structure of R6G, the electronic transition dipole (along the long axis when excited at 514.5 nm), and the dichroic polarizer orientations. Other conditions as in Fig. 3.

experimental conditions (Fig. 6). The fluorescence signals arise from R6G molecules that are directly attached to the dielectric glass surface and whose fluorescence quantum yields (~0.8) are only slightly lower than that in ethanol solution (*7*). The Raman signals are from dye molecules that are adsorbed on the Ag metal particles, and their fluorescence is quenched. To prevent exchange between free and adsorbed R6G molecules, we incubated the Ag colloid with R6G and then rapidly dispersed and dried it on a glass cover slip. Because R6G fluorescence and Raman spectra overlap in the spectral range 540 to 580 nm (Stokes shift, 920 to 2200 cm^{-1}), we used a single bandpass filter (centered at 560 nm; full width at half maximum, 40 nm) to record integrated fluorescence and Raman signals in this 40-nm spectral region. However, a continuous background emission is commonly observed in SERS (*14*), and the integrated Raman signal contains a large background component (as high as 80% of the overall signal). After careful, pixel-by-pixel background subtraction, we estimate that the Raman signals are about four to five times higher than the integrated fluorescence of single R6G molecules.

We attribute the large enhancement factors to the removal of two population-averaging effects. Conventional measurements over a large ensemble of molecules and particles yield population-averaged results, because all molecules and particles are assumed to contribute equally to the observed signals. The intrinsic enhancement effect can be 10^6 to 10^7 times larger than the ensemble-averaged value, because only one out of perhaps 100 to 1000 particles is optically hot (a particle-averaging factor of 10^2 to 10^3) and only one out of 10,000 surface sites on a hot particle shows efficient enhancement (a molecule-averaging factor of 10^4). These estimates are based on the observed percentage of hot particles as well as the maximum number of R6G molecules (about 1.8×10^4) adsorbed on an average particle at monolayer coverage.

Consistent with this explanation, other researchers have reported unusually large enhancement factors when statistical averaging is reduced under special conditions. Hildebrandt and Stockburger (*19*) obtained SERS spectra of R6G adsorbed on colloidal Ag at very low concentrations (~10^{-11} M), at which the molecule-averaging effect should be significantly reduced. Their results indicate that the enhanced Raman scattering efficiencies can approach those of R6G fluorescence and that each colloidal particle contains an average of only 3.3 adsorption sites that are especially efficient for enhancement. This limited number of active sites agrees with our own observation that the surface Raman signals of citrate ions are completely suppressed at a R6G concentration higher than 10^{-10} M. In a different study, Kneipp *et al.* (*23*) used SERS for efficient pumping of the excited vibrational states of R6G adsorbed on colloidal Ag. The observed Raman signals appear to be dominated by as low as 0.01% of the adsorbed molecules, and the Raman scattering cross sections could be as large as 10^{-16} cm^2 per molecule. For surface-enhanced nonlinear optical processes such as hyper-Raman scattering, Van Duyne and co-workers (*24*) have reported enhancement factors for pyridine on the order of ~10^{13}.

Optimization of the colloid-preparation and activation procedures should allow SERS single-molecule studies of a broader range of systems such as nonfluorescent hemoproteins, nucleotides, and pyridyl compounds. The resonance-enhancement effect, which is present in the R6G spectra excited at 514.5 nm, may not be necessary because surface enhancement is clearly the dominant factor. For better control of particle size and shape, Ag and Au nanostructures could be prepared by electrochemical deposition with a scanning tunneling microscope (STM) (*25*), synthesis in the pores of nanoporous membranes (*26*), and metal vapor deposition on latex nanospheres (*27*). Recently, Sun and co-workers used STM-directed lithography to fabricate micrometer-sized Ag particles and measured the optical properties of single particles (*28*).

The methods and instrumentation of this report also open the possibility of studying the size-dependent properties of single organic nanostructures (*26*) and semiconductor nanocrystals (*29*). Single CdSe quantum dots have been shown (*30*) to emit luminescent light intermittently with a characteristic time scale of about 0.5 s. This intermittency has been suggested to arise from photoionization and charge neutralization of the semiconductor nanocrystal. However, our time-resolved studies of individual, hot Ag nanoparticles also reveal an irregular on and off photon emission behavior on a similar time scale. In these Ag metal particles, photogeneration of electron-hole pairs is not possible, and light emission arises from SERS, not photoluminescence. Further research should yield important insights into the intrinsic properties of single molecules and nanostructures.

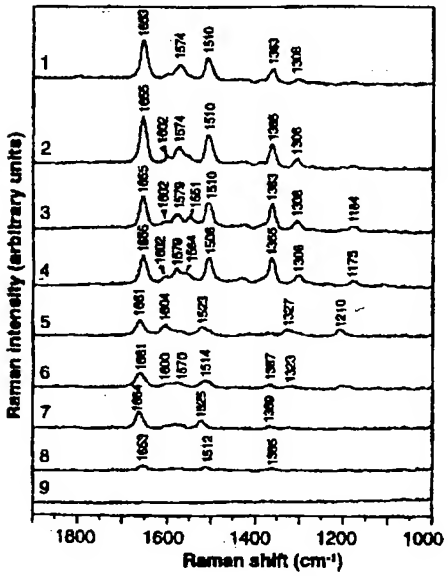

Fig. 5. Time-resolved surface-enhanced Raman spectra of a single R6G molecule recorded at 1-s intervals. Over 300 spectra were recorded from this particular particle before the signals disappeared. Nine spectra were selected to highlight sudden spectral changes. The Raman signals abruptly changed in both frequency and intensity three times, as shown in spectra 2, 5, and 8. The laser excitation power was about 10 μW, and other conditions were as in Fig. 3.

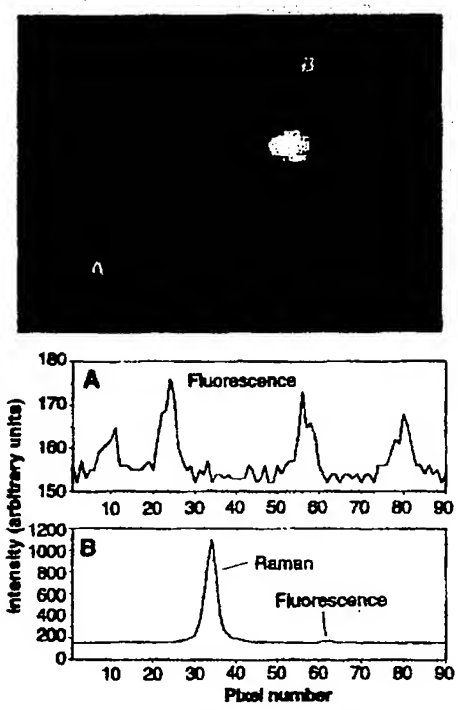

Fig. 6. Direct comparison of laser-induced fluorescence and SERS of a single R6G molecule. Note that single-molecule fluorescence signals were observed as diffraction-limited spots (~500 nm in diameter or 6 pixels). The integrated Raman signal appeared much larger in size, but its full width at half maximum was similar to that for fluorescence. Detailed signal intensities and widths are shown for lines (**A**) and (**B**). Laser wavelength, 514.5 nm; excitation power, 10 mW; integration time, 5 s.

REFERENCES AND NOTES

1. For recent reviews, see W. E. Moerner, *Science* **265**, 46 (1994); J. L. Skinner and W. E. Moerner, *J. Phys. Chem.* **100**, 13251 (1996).
2. M. Orrit, J. Bernard, R. I. Personov, *J. Phys. Chem.* **97**, 10256 (1993).

3. F. Guttler, T. Irngartinger, T. Plakhotnik, A. Renn, U. P. Wild, *Chem. Phys. Lett.* **217**, 393 (1994).
4. E. B. Shera, N. K. Seitzinger, L. M. Davis, R. A. Keller, S. A. Soper, *ibid.* **174**, 553 (1990); M. D. Barnes, K. C. Ng, W. B. Whitten, J. M. Ramsey, *Anal. Chem.* **65**, 2360 (1993).
5. M. Eigen and R. Rigler, *Proc. Natl. Acad. Sci. U.S.A.* **91**, 5740 (1994); S. Nie, D. T. Chiu, R. N. Zare, *Science* **266**, 1018 (1994).
6. E. Betzig and R. J. Chichester, *Science* **262**, 1422 (1993); X. S. Xie and R. C. Dunn, *ibid.* **265**, 361 (1994).
7. W. P. Ambrose, P. M. Goodwin, J. C. Martin, R. A. Keller, *ibid.* **265**, 364 (1994); *Phys. Rev. Lett.* **72**, 160 (1994).
8. J. K. Trautman, J. J. Macklin, L. E. Brus, E. Betzig, *Nature* **369**, 40 (1994); J. J. Macklin, J. K. Trautman, T. D. Harris, L. E. Brus, *Science* **272**, 255 (1996).
9. T. Ha *et al.*, *Proc. Natl. Acad. Sci. U.S.A.* **93**, 6264 (1996).
10. R. A. Keller *et al.*, *Appl. Spectrosc.* **50** (no. 7), 12A (1996); S. Nie and R. N. Zare, *Annu. Rev. Biophys. Biomol. Struct.*, in press.
11. T. Funatsu, Y. Harada, M. Tokunaga, K. Saito, T. Yanagida, *Nature* **374**, 555 (1995).
12. Th. Schmidt, G. J. Schutz, W. Baumgartner, H. J. Gruber, H. Schindler, *Proc. Natl. Acad. Sci. U.S.A.* **93**, 2926 (1996); Q. Xue and E. S. Yeung, *Nature* **373**, 681 (1995); A. Castro, F. R. Fairfield, E. B. Shera, *Anal. Chem.* **65**, 849 (1993); B. B. Haab and R. A. Mathies, *ibid.* **67**, 3253 (1995).
13. F.-R. F. Fan and A. J. Bard, *Science* **267**, 871 (1995); M. M. Collinson and R. M. Wightman, *ibid.* **268**, 1883 (1995).
14. For reviews, see M. Moskovits, *Rev. Mod. Phys.* **57**, 783 (1985); A. Otto, I Mrozek, H. Grabhorn, W. Akemann, *J. Phys. Condens. Matter* **4**, 1143 (1992); G. C. Schatz, *Acc. Chem. Res.* **17**, 370 (1984).
15. A. B. Meyers, P. Tchenio, M. Z. Zgierski, W. E. Moerner, *J. Phys. Chem.* **98**, 10377 (1994); J. Fleury, Ph. Tamarat, B. Lounis, J. Bernard, M. Orrit, *Chem. Phys. Lett.* **236**, 87 (1995).
16. K. Kneipp *et al.*, abstract 24 presented at the 23rd Annual Conference of the Federation of Analytical Chemistry and Spectroscopy Societies, Kansas City, MO, 29 September to 4 October 1996.
17. A 250-μl aliquot of Ag colloid prepared by the procedure of P. C. Lee and D. Meisel [*J. Phys. Chem.* **86**, 3391 (1982)] was incubated with R6G and ~1 mM NaCl in a 1.5-ml plastic microcentrifuge tube. Glass containers should be avoided because of R6G adsorption on glass surfaces. At the electrolyte concentrations used, the Ag colloid was activated, but not aggregated, after an extended incubation time of ~3 hours at room temperature. The amount of free R6G in solution was experimentally determined to be ~20% by centrifugation of the Ag particles and fluorescence measurement of the supernatant solution. This result is in agreement with the calculated value (~10 to 20%) based on the equilibrium binding constant 1.8×10^{-9} M (*19*). Bulk R6G concentrations from 10^{-7} to 10^{-11} M were calibrated by fluorescence measurement in the absence of Ag colloids. The order, speed, and buffer volume of the colloid-analyte mixing process did not make measurable differences, indicating that equilibrium adsorption conditions were reached in our experiment.
18. R. G. Freeman *et al.*, *Science* **267**, 1629 (1995); G. Chumanov, K. Sokolov, B. W. Gregory, T. M. Cotton, *J. Phys. Chem.* **99**, 9466 (1995).
19. P. Hildebrandt and M. Stockburger, *J. Phys. Chem.* **88**, 5935 (1984).
20. In this integrated microscope, ultrasensitive optical imaging and spectroscopy provided molecular information, and AFM resolved the shape and size of individual nanoparticles. The microscope side port was coupled to a high-throughput, single-stage spectrograph and a back-illuminated charge-coupled device (CCD) detector for spectroscopy. The microscope front was attached to a video-rate intensified CCD for wide-field imaging of single nanoparticles with epi- or evanescent-wave laser excitation. A tapping-mode AFM scanning head was mounted directly on the microscope stage for topographic imaging at nanometer-scale resolution. When coupled with a video data acquisition system, this apparatus allowed digital movies to be made of single nanoparticles at 30 frames per second. Detailed instrument diagram and specifications are available upon request.
21. This question can be addressed by using near-field scanning optical microscopy to image nanoparticle aggregates at a resolution of 50 to 100 nm. Recent research shows that both surface and resonance-enhanced Raman spectra can be obtained with a near-field fiber probe in nanometer domains [S. R. Emory and S. Nie, in *International Conference on Raman Spectroscopy*, S. A. Asher and P. B. Stein, Eds. (Wiley, New York, 1996), pp. 1176–1177; S. Webster, D. A. M. Smith, M. W. Ayad, K. Kershaw, D. N. Batchelder, *ibid.*, pp. 1146–1147].
22. H. Jakobi and H. Kuhn, *Ber. Bunsenges. Phys. Chem.* **66**, 46 (1962).
23. K. Kneipp *et al.*, *Phys. Rev. Lett.* **76**, 2444 (1996).
24. J. T. Golab, J. R. Sprague, K. T. Carron, G. C. Schatz, R. P. Van Duyne, *J. Chem. Phys.* **88**, 7942 (1988).
25. W. Li, J. A. Virtanen, R. M. Penner, *J. Phys. Chem.* **96**, 6529 (1992); *ibid.* **98**, 11751 (1994).
26. C. R. Martin, *Science* **266**, 1961 (1994); *Acc. Chem. Res.* **28**, 61 (1995).
27. R. P. Van Duyne, J. C. Hulteen, D. A. Treichel, *J. Chem. Phys.* **99**, 2101 (1993).
28. T. Xiao, Q. Ye, L. Sun, *J. Phys. Chem.*, in press.
29. A. P. Alivisatos, *Science* **271**, 933 (1996); *J. Phys. Chem.* **100**, 13226 (1996).
30. M. Nirmal *et al.*, *Nature* **383**, 802 (1996).

31. S.N. acknowledges the Whitaker Foundation for a Biomedical Engineering Award and the Beckman Foundation for a Beckman Young Investigator Award. This work was supported by Indiana University Startup Funds.

1 November 1996; accepted 17 December 1996

Direct Measurement of Single-Molecule Diffusion and Photodecomposition in Free Solution

Xiao-Hong Xu and Edward S. Yeung*

Continuous monitoring of submillisecond free-solution dynamics of individual rhodamine-6G molecules and 30-base single-stranded DNA tagged with rhodamine was achieved. Fluorescence images were recorded from the same set of isolated molecules excited either through the evanescent field at the quartz-liquid interface or as a thin layer of solution defined by micron-sized wires, giving diffraction-limited resolution of interconnected attoliter volume elements. The single-molecule diffusion coefficients were smaller and the unimolecular photodecomposition lifetimes were longer for the dye-DNA covalent complex as compared with those of the dye molecule itself. Unlike bulk studies, stochastic behavior was found for individual molecules of each type, and smaller diffusion coefficients were observed.

A variety of approaches have recently been demonstrated for single-molecule detection (SMD) (*1–9*). SMD is a way to study and characterize detailed physical and chemical properties that allows the testing of fundamental principles and may lead to technological and methodological developments with applications in medicine, biotechnology, and molecular biology (*5*, *8*, *10*). The detection of single molecules in solution has become relatively straightforward. However, continuous monitoring of a single molecule in free solution remains a challenge (*6–9*, *11*). We report here that real-time observation of individual rhodamine-6G (R6G) and rhodamine-labeled 30-base single-stranded DNA (ssDNA) (DNA-R6G) (*12*) molecules in water solution can be achieved by the simple combination of an optical microscope and an intensified charge-coupled device (ICCD) camera. Depending on the arrangement, molecular dynamics either at the quartz-liquid interface or in the bulk liquid can be followed with submillisecond time resolution.

To increase the signal-to-noise ratio in SMD, one can reduce the observation volume (*2*, *6*, *13*), thereby increasing the effective concentration of the molecule of interest. Miniaturization helps to isolate individual molecules, allowing the signal to be assigned to distinct entities. However, fixing a small observation volume and allowing a molecule to diffuse into and out of the region requires either statistics (*5*) or deconvolution with respect to the many possible paths (*7*) in order to extract molecular motion and other kinetic information. One must follow the same molecule continuously because assembly of a large number of single-molecule signals for interpretation (*11*) cannot reveal characteristic differences among molecules as opposed to just mapping out the shape of the probability distribution. The data rate is important in free solution because confinement such as that provided by rigid media (*4*), lipid membranes (*14*), or gel matrices (*15*) is not available. These requirements suggest the

Ames Laboratory–U.S. Department of Energy and Department of Chemistry, Iowa State University, Ames, IA 50011, USA.

*To whom correspondence should be addressed.